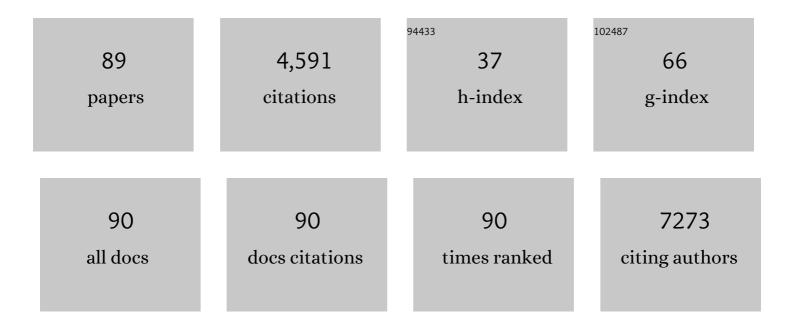
Luhua Lu

List of Publications by Year in descending order

Source: https://exaly.com/author-pdf/8458608/publications.pdf Version: 2024-02-01



Тиникти

#	Article	IF	CITATIONS
1	Heterostructure nanocomposite with local surface plasmon resonance effect enhanced photocatalytic activity—a critical review. Journal Physics D: Applied Physics, 2022, 55, 043002.	2.8	13
2	Constructing two dimensional composite nanosheets with montmorillonite and graphene-like carbon: Towards high-rate-performance PVA based gel polymer electrolytes for quasi-solid-state supercapacitors. Materials Chemistry and Physics, 2022, 287, 126333.	4.0	4
3	Montmorillonite as the multifunctional reagent for preparing reduced graphene oxide and its improved supercapacitive performance. Applied Clay Science, 2021, 200, 105821.	5.2	3
4	Nitrogen-doped graphene/graphitic carbon nitride with enhanced charge separation and two-electron-transferring reaction activity for boosting photocatalytic hydrogen peroxide production. Sustainable Energy and Fuels, 2021, 5, 1511-1520.	4.9	13
5	Dualâ€Responsive Soft Actuators with Integrated Sensing Function Based on 1Tâ€MoS ₂ Composite. Advanced Intelligent Systems, 2021, 3, 2000240.	6.1	15
6	Carbon nitride derived carbon and nitrogen Co-doped CdS for stable photocatalytic hydrogen evolution. Surfaces and Interfaces, 2021, 25, 101262.	3.0	11
7	Comparative tribological behavior of friction composites containing natural graphite and expanded graphite. Friction, 2020, 8, 684-694.	6.4	18
8	3D printing-based cellular microelectrodes for high-performance asymmetric quasi-solid-state micro-pseudocapacitors. Journal of Materials Chemistry A, 2020, 8, 1749-1756.	10.3	35
9	Boosting electrocatalytic oxygen evolution using ultrathin carbon protected iron–cobalt carbonate hydroxide nanoneedle arrays. Journal of Power Sources, 2020, 450, 227639.	7.8	23
10	Carbon nanotube exfoliated porous reduced graphene oxide/CdS- diethylenetriamine heterojunction for efficient photocatalytic H2 production. Applied Surface Science, 2020, 512, 144783.	6.1	26
11	Effect of CaO and CeO ₂ co-doping on thermo-physical properties of La ₂ Z ₂ O ₇ . Journal of Asian Ceramic Societies, 2020, 8, 1010-1017.	2.3	3
12	Nitrogenâ€doped Graphene Chainmail Wrapped IrCo Alloy Particles on Nitrogenâ€doped Graphene Nanosheet for Highly Active and Stable Full Water Splitting. ChemCatChem, 2019, 11, 5457-5465.	3.7	20
13	Graphene edge-enhanced anchoring of the well-exposed cobalt clusters <i>via</i> strong chemical bonding for accelerating the oxygen reduction reaction. Sustainable Energy and Fuels, 2019, 3, 2859-2866.	4.9	6
14	Inorganic-organic CdSe-diethylenetriamine nanobelts for enhanced visible photocatalytic hydrogen evolution. Journal of Colloid and Interface Science, 2019, 555, 166-173.	9.4	44
15	Commercial-Level Energy Storage via Free-Standing Stacking Electrodes. Matter, 2019, 1, 1694-1709.	10.0	19
16	Revealing important role of graphitic carbon nitride surface catalytic activity in photocatalytic hydrogen evolution by using different carbon co-catalysts. Applied Surface Science, 2019, 491, 236-244.	6.1	14
17	Preparation of Z-scheme WO3(H2O)0.333/Ag3PO4 composites with enhanced photocatalytic activity and durability. Chinese Journal of Catalysis, 2019, 40, 326-334.	14.0	55
18	Biological Visual Detection for Advanced Photocatalytic Oxidation toward Pesticide Detoxification. ACS Omega, 2019, 4, 19655-19663.	3.5	4

Lиниа Lu

#	Article	IF	CITATIONS
19	Pseudocapacitive Co9S8/graphene electrode for high-rate hybrid supercapacitors. Carbon, 2019, 141, 134-142.	10.3	110
20	Rapid adsorption of cationic dye-methylene blue on the modified montmorillonite/graphene oxide composites. Applied Clay Science, 2019, 168, 304-311.	5.2	67
21	Construction of defective Mo15S19/CdS-diethylenetriamine heterosctructure photocatalyst for highly active and stable noble-metal-free photocatalytic hydrogen production. Applied Surface Science, 2019, 469, 505-513.	6.1	37
22	Biomass chitosan derived cobalt/nitrogen doped carbon nanotubes for the electrocatalytic oxygen reduction reaction. Journal of Materials Chemistry A, 2018, 6, 5740-5745.	10.3	113
23	Porous carbon nitride with defect mediated interfacial oxidation for improving visible light photocatalytic hydrogen evolution. Applied Catalysis B: Environmental, 2018, 232, 384-390.	20.2	62
24	Tuning active sites on cobalt/nitrogen doped graphene for electrocatalytic hydrogen and oxygen evolution. Electrochimica Acta, 2018, 265, 497-506.	5.2	56
25	A green method to reduce graphene oxide with carbonyl groups residual for enhanced electrochemical performance. Carbon, 2018, 133, 101-108.	10.3	25
26	Natural nanomaterial as hard template for scalable synthesizing holey carbon naonsheet/nanotube with in-plane and out-of-plane pores for electrochemical energy storage. Chinese Chemical Letters, 2018, 29, 641-644.	9.0	4
27	Boosting visible light photocatalytic hydrogen evolution of graphitic carbon nitride via enhancing it interfacial redox activity with cobalt/nitrogen doped tubular graphitic carbon. Applied Catalysis B: Environmental, 2018, 225, 512-518.	20.2	65
28	Sustainable synthesis of CeO 2 /CdS-diethylenetriamine composites for enhanced photocatalytic hydrogen evolution under visible light. Journal of Alloys and Compounds, 2018, 758, 162-170.	5.5	54
29	Manipulation structure of carbon nitride via trace level iron with improved interfacial redox activity and charge separation for synthetic enhancing photocatalytic hydrogen evolution. Applied Surface Science, 2018, 456, 609-614.	6.1	13
30	Recent progress on band and surface engineering of graphitic carbon nitride for artificial photosynthesis. Applied Surface Science, 2018, 462, 693-712.	6.1	51
31	Non-equilibrium microstructure of Li1.4Al0.4Ti1.6(PO4)3 superionic conductor by spark plasma sintering for enhanced ionic conductivity. Nano Energy, 2018, 51, 19-25.	16.0	24
32	In situ controllable synthesis of novel surface plasmon resonance-enhanced Ag 2 WO 4 /Ag/Bi 2 MoO 6 composite for enhanced and stable visible light photocatalyst. Applied Surface Science, 2017, 391, 507-515.	6.1	123
33	Graphitic carbon nitride nanosheet for photocatalytic hydrogen production: The impact of morphology and element composition. Applied Surface Science, 2017, 391, 369-375.	6.1	88
34	Residual oxygen groups in nitrogen-doped graphene to enhance the capacitive performance. RSC Advances, 2017, 7, 15293-15301.	3.6	22
35	Morphology dependent adsorption of methylene blue on trititanate nanoplates and nanotubes prepared by the hydrothermal treatment of TiO2. Water Science and Technology, 2017, 75, 350-357.	2.5	1
36	Multi-walled carbon nanotube supported CdS-DETA nanocomposite for efficient visible light photocatalysis. Materials Chemistry and Physics, 2017, 186, 372-381.	4.0	39

Lиниа Lu

#	Article	lF	CITATIONS
37	Cu/Ag/Ag3PO4 ternary composite: A hybrid alloy-semiconductor heterojunction structure with visible light photocatalytic properties. Journal of Alloys and Compounds, 2016, 682, 778-784.	5.5	27
38	Phosphoric acid-assisted synthesis of layered MoS ₂ /graphene hybrids with electrolyte-dependent supercapacitive behaviors. RSC Advances, 2016, 6, 89397-89406.	3.6	12
39	Buffering agents-assisted synthesis of nitrogen-doped graphene with oxygen-rich functional groups for enhanced electrochemical performance. Journal of Power Sources, 2016, 333, 125-133.	7.8	31
40	Impact of size on energy storage performance of graphene based supercapacitor electrode. Electrochimica Acta, 2016, 219, 463-469.	5.2	32
41	Carbon Nitride Supramolecular Hybrid Material Enabled High-Efficiency Photocatalytic Water Treatments. Nano Letters, 2016, 16, 6568-6575.	9.1	108
42	Highly defective graphite for scalable synthesis of nitrogen doped holey graphene with high volumetric capacitance. Journal of Power Sources, 2016, 334, 104-111.	7.8	30
43	A facile fabrication of plasmonic g-C 3 N 4 /Ag 2 WO 4 /Ag ternary heterojunction visible-light photocatalyst. Materials Chemistry and Physics, 2016, 177, 529-537.	4.0	75
44	Large-scale synthesis of cobalt sulfide/carbon nanotube hybrid and its excellent electrochemical capacitance performance. Materials Letters, 2016, 176, 42-45.	2.6	21
45	Hydrothermal synthesis of layered molybdenum sulfide/N-doped graphene hybrid with enhanced supercapacitor performance. Carbon, 2016, 99, 35-42.	10.3	183
46	Large scale and facile synthesis of novel Z-scheme Bi2MoO6/Ag3PO4 composite for enhanced visible light photocatalyst. Materials Letters, 2016, 169, 250-253.	2.6	36
47	A Graphene-like Oxygenated Carbon Nitride Material for Improved Cycle-Life Lithium/Sulfur Batteries. Nano Letters, 2015, 15, 5137-5142.	9.1	358
48	Facile and large scale synthesis of novel Cu2O octahedral crystals with efficient visible light photocatalytic activity. Materials Letters, 2015, 150, 48-51.	2.6	23
49	A high efficient graphitic-C ₃ N ₄ /BiOI/graphene oxide ternary nanocomposite heterostructured photocatalyst with graphene oxide as electron transport buffer material. Dalton Transactions, 2015, 44, 7903-7910.	3.3	149
50	Advance ternary surface-fluorinated TiO ₂ nanosheet/Ag ₃ PO ₄ /Ag composite photocatalyst with planar heterojunction and island Ag electron capture center. RSC Advances, 2014, 4, 62751-62758.	3.6	13
51	A scalable synthesis technique of hierarchical BiOBr microspheres for advanced visible light photocatalyst. Materials Letters, 2014, 136, 438-440.	2.6	13
52	Synthesis of micro-nano heterostructure AgBr/ZnO composite for advanced visible light photocatalysis. Materials Letters, 2014, 130, 5-8.	2.6	48
53	High-yield synthesis of carbon nanotube–porous nickel oxide nanosheet hybrid and its electrochemical capacitance performance. Materials Chemistry and Physics, 2014, 143, 1344-1351.	4.0	27
54	The stabilization effect of surface capping on photocatalytic activity and recyclable stability of Ag3PO4. Catalysis Communications, 2014, 46, 138-141.	3.3	21

Lиниа Lu

#	Article	IF	CITATIONS
55	In situ assembly of MnO2 nanowires/graphene oxide nanosheets composite with high specific capacitance. Electrochimica Acta, 2014, 116, 111-117.	5.2	95
56	Enhanced electrochemical energy storage performance of reduced graphene oxide by incorporating oxygen-rich in-plane pores. Journal of Materials Chemistry A, 2014, 2, 1802-1808.	10.3	18
57	Graphene oxide capturing surface-fluorinated TiO ₂ nanosheets for advanced photocatalysis and the reveal of synergism reinforce mechanism. Dalton Transactions, 2014, 43, 2202-2210.	3.3	66
58	Facile synthesis of a reduced graphene oxide/cobalt sulfide hybrid and its electrochemical capacitance performance. RSC Advances, 2014, 4, 29216-29222.	3.6	37
59	Heterojunction of facet coupled g-C3N4/surface-fluorinated TiO2 nanosheets for organic pollutants degradation under visible LED light irradiation. Applied Catalysis B: Environmental, 2014, 156-157, 331-340.	20.2	316
60	Plasmonic TiO 2 /AgBr/Ag ternary composite nanosphere with heterojunction structure for advanced visible light photocatalyst. Applied Surface Science, 2014, 314, 864-871.	6.1	44
61	A facile surfactant-free method to prepare Ti0.95Er0.05O2 nanocrystal and its photocatalytic performance. Catalysis Communications, 2014, 43, 202-206.	3.3	9
62	Graphene oxide modified ZnO nanorods hybrid with high reusable photocatalytic activity under UV-LED irradiation. Materials Chemistry and Physics, 2014, 143, 1410-1416.	4.0	60
63	Sonication assisted preparation of graphene oxide/graphitic-C3N4 nanosheet hybrid with reinforced photocurrent for photocatalyst applications. Dalton Transactions, 2014, 43, 6295.	3.3	178
64	Development of UV-LED/TiO2 Device and Their Application for Photocatalytic Degradation of Methylene Blue. Journal of Materials Engineering and Performance, 2013, 22, 1035-1040.	2.5	45
65	Superhydrophilic zinc oxide film prepared by controlling ZnO microrods growth and its attractive recyclable photocatalytic performance. Thin Solid Films, 2013, 539, 23-28.	1.8	6
66	Taking the place of perylene diimide: perylene tetracarboxylic tetraester as a building block for polymeric acceptors to achieve higher open circuit voltage in all-polymer bulk heterojunction solar cells. Polymer Chemistry, 2013, 4, 5612.	3.9	52
67	Facile synthesis of a surface plasmon resonance-enhanced Ag/AgBr heterostructure and its photocatalytic performance with 450 nm LED illumination. Dalton Transactions, 2013, 42, 4657.	3.3	64
68	Graphene‣tabilized Silver Nanoparticle Electrochemical Electrode for Actuator Design. Advanced Materials, 2013, 25, 1270-1274.	21.0	130
69	Tuning optical and electronic properties of star-shaped conjugated molecules with enlarged Ï€-delocalization for organic solar cell application. Journal of Materials Chemistry A, 2013, 1, 8270.	10.3	45
70	Mass Production and Reusable Photocatalytic Activity of ZnS Microspheres. Nanoscience and Nanotechnology Letters, 2013, 5, 204-208.	0.4	0
71	Large volume variation of an anisotropic graphene nanosheet electrochemical–mechanical actuator under low voltage stimulation. Chemical Communications, 2012, 48, 3978.	4.1	43
72	A scalable synthesis technique of novel AgBr microcrystal and its visible light photocatalytic performance. Materials Letters, 2012, 87, 94-96.	2.6	18

Luниа Lu

#	Article	IF	CITATIONS
73	Actuators: Highly Stable Air Working Bimorph Actuator Based on a Graphene Nanosheet/Carbon Nanotube Hybrid Electrode (Adv. Mater. 31/2012). Advanced Materials, 2012, 24, 4222-4222.	21.0	0
74	Direct growth of size-controlled gold nanoparticles on reduced graphene oxide film from bulk gold by tuning electric field: effective methodology and substrate for surface enhanced Raman scattering study. Journal of Materials Chemistry, 2012, 22, 11994.	6.7	34
75	Self-regenerated solar-driven photocatalytic water-splitting by urea derived graphitic carbon nitride with platinum nanoparticles. Chemical Communications, 2012, 48, 8826.	4.1	244
76	Highly Stable Air Working Bimorph Actuator Based on a Graphene Nanosheet/Carbon Nanotube Hybrid Electrode. Advanced Materials, 2012, 24, 4317-4321.	21.0	125
77	Dopamineâ€Modified Trititanate Nanotubes with UV―and Visibleâ€Light Photocatalytic Activity: Coordinative Selfâ€Assembly into a Recyclable Absorber. ChemCatChem, 2012, 4, 1133-1138.	3.7	11
78	Large scale preparing carbon nanotube/zinc oxide hybrid and its application for highly reusable photocatalyst. Chemical Engineering Journal, 2012, 191, 571-578.	12.7	127
79	Ring formation mechanism of single-walled carbon nanotubes: Energy conservation between curvature elasticity and inter-tube adhesion. Chemical Physics, 2012, 393, 123-128.	1.9	4
80	Facile preparation and growth mechanism of zinc oxide nanopencils. Materials Letters, 2012, 67, 193-195.	2.6	12
81	Easy and Large Scale Synthesis Silver Nanodendrites: Highly Effective Filler for Isotropic Conductive Adhesives. Journal of Materials Engineering and Performance, 2012, 21, 353-357.	2.5	7
82	Bending Deformation Mechanism and Defective Properties of Liquid Crystalline Carbon Nanotubes in Evaporating Droplets. RSC Advances, 2011, 1, 468.	3.6	5
83	Supramolecular self-assembly of biopolymers with carbon nanotubes for biomimetic and bio-inspired sensing and actuation. Nanoscale, 2011, 3, 2412.	5.6	26
84	Biocompatible Composite Actuator: A Supramolecular Structure Consisting of the Biopolymer Chitosan, Carbon Nanotubes, and an Ionic Liquid. Advanced Materials, 2010, 22, 3745-3748.	21.0	114
85	Bionic nanocomposite actuator based on carbon nanotube and ionic biopolymer. , 2010, , .		0
86	Large-Scale Aligned Carbon Nanotubes from Their Purified, Highly Concentrated Suspension. ACS Nano, 2010, 4, 1042-1048.	14.6	70
87	Electromechanical Actuation with Controllable Motion Based on a Single-Walled Carbon Nanotube and Natural Biopolymer Composite. ACS Nano, 2010, 4, 3498-3502.	14.6	98
88	Carbon Nanotubes Engineering Assisted by Natural Biopolymers. , 0, , .		0
89	A Costâ€Effective Iron Based COF and Its Composite Electrocatalyst for Active and Stable Oxygen Reduction Reaction In Alkaline Solution. ChemElectroChem, 0, , .	3.4	1